ACS Photonics

Article

pubs.acs.org/journal/apchd5

Impact of the Nature of the Excited-State Transition Dipole Moments on the Third-Order Nonlinear Optical Response of Polymethine Dyes for All-Optical Switching Applications

Rebecca L. Gieseking, Sukrit Mukhopadhyay,† Chad Risko, and Jean-Luc Brédas*

School of Chemistry and Biochemistry and Center for Organic Materials for All-Optical Switching, Georgia Institute of Technology, Atlanta, Georgia 30332-0400, United States

Supporting Information

ABSTRACT: Designing molecular materials with the figures-of-merit needed for all-optical switching applications requires that, at the wavelengths of interest, the molecules have large real components |Re(γ)| of the third-order polarizability (γ) while at the same time maintaining small imaginary components Im(γ). Polymethines have the potential to meet these conditions, though to date only a few polymethines exhibit large enough |Re(γ)/Im(γ)| for device applications. From the sum-over-states expression for γ, it can be deduced that when the transition dipole moment ($\mu_{ee'}$) between the polymethine first and second excited states is minimized, Im(γ) decreases and |Re(γ)| increases. Here, focusing on a series of streptocyanines, we decompose $\mu_{ee'}$ into the transition dipole components of the constituent electronic transitions and investigate how variations in chain length and substitution patterns alter $\mu_{ee'}$. The second, two-photon-allowed, excited state is shown to be composed primarily of three excitations, two of which contribute to $\mu_{ee'}$ in an additive fashion, while the third reduces the magnitude of $\mu_{ee'}$. As the conjugation path length growths, the competition between two factors, (i) the increased wave function overlap in each constituent transition vs (ii) the increased influence of the electronic configuration with a negative contribution to $\mu_{ee'}$, results in a weak dependence of $\mu_{ee'}$ on length. Electron-donating and -withdrawing substituents are shown to affect $\mu_{ee'}$ by influencing the energetic spacing of the first few frontier molecular orbitals, which offers a path for further tuning of $\mu_{ee'}$; in particular, it is found that a large energetic spacing between the HOMO−1 and HOMO levels and between the LUMO and LUMO+1 levels is a critical feature to achieve small $\mu_{ee'}$ values.

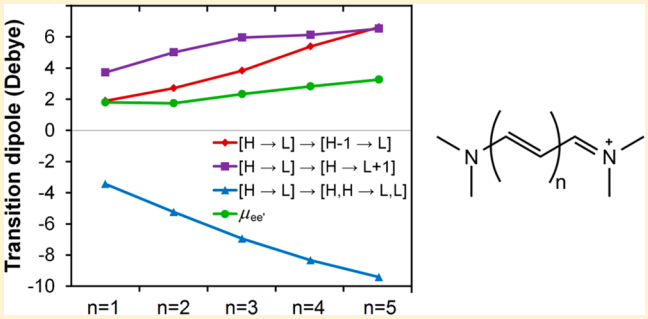

KEYWORDS: *cyanines/polymethines, transition dipole moment, nonlinear optics, all-optical switching*

The demand for data transmission is escalating at a tremendous pace as a result of the cumulative rise in tele-/videocommunications, cloud computing, video and music streaming, and the upsurge in use of mobile devices (e.g., smart phones, tablets), among many factors.[1] To meet future requirements, it is estimated that optical switches within the fiber optic framework will need to operate at rates faster than 1 terabit/s,[2] an order of magnitude faster than current optoelectrical switches within the telecommunications wavelength window (λ = 1300−1550 nm; $\hbar\omega$ = 0.95−0.8 eV).[3] All-optical switching (AOS) interconnects provide opportunities to meet these demands.[4−6] In an all-optical switch, an incoming optical "data" signal is manipulated by a second optical "switching" signal (without the need for any electrical signal) via the interaction of the light with a photonic material with a sizable third-order nonlinear optical (NLO) response. For efficient AOS, at a given wavelength, the photonic material must (i) possess a large nonlinear refractive index, which is directly proportional to the real component, Re(γ), of the third-order polarizability, γ, and (ii) have minimal two-photon absorption (TPA) losses, which are directly proportional to the imaginary component of γ, Im(γ). The figure of merit (FOM), defined as |Re(γ)/Im(γ)|, is required to be greater than 4π for a switch to be considered functional.[7]

Organic π-conjugated materials have long held interest for a wide variety of NLO applications,[8−13] with polyenes (i.e., conjugated molecules with an even number of sp^2-hybridized CH groups) and polymethines (i.e., conjugated molecules with an odd number of sp^2-hybridized CH groups) serving as prototypical materials for many fundamental and applied studies (Figure 1). In these systems, the first two excited states are the 1B-type state (e), which has a large one-photon absorption (OPA) cross-section, and the 2A-type state (e'), which is two-photon allowed. Importantly (see Figure 1), the order of these states differs in the two molecular classes: in polymethines, the energy $E_{ge'}$ of the 2A state e' is substantially larger than the energy E_{ge} of state e,[14,15] whereas in polyenes longer than butadiene $E_{ge'}$ is slightly smaller than E_{ge}.[16−19] The

Received: November 27, 2013
Published: February 24, 2014

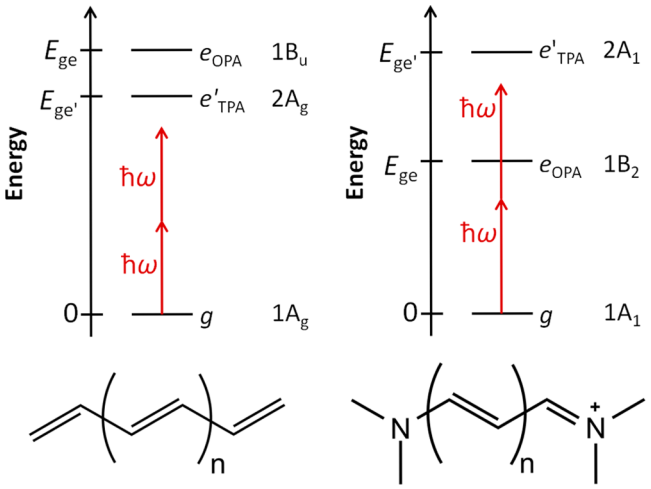

Figure 1. Energy-level diagrams and chemical structures for polyenes (left) and the polymethines commonly known as streptocyanines (right). Here, we consider molecular lengths of n = 1−5 and substitution with $-OCH_3$ or $-CF_3$ groups on the central carbon atom of the streptocyanines and the central two carbon atoms of the polyenes.

large energetic spacing between states e and e' in polymethines imparts the potential for large AOS figures-of-merit when the incoming optical data signals are at an energy $\hbar\omega$ such that $E_{ge} < 2\hbar\omega < E_{ge'}$. In this situation, $|\mathrm{Re}(\gamma)|$ can exhibit significant preresonant enhancement because of the small energy difference between $\hbar\omega$ and E_{ge} without incurring significant losses due to TPA.[20] In polyenes by contrast, $2\hbar\omega$ must be smaller than $E_{ge'}$ to avoid significant TPA losses, which does not allow for significant preresonant enhancement of $\mathrm{Re}(\gamma)$. While we note that the FOM in polymethines depends on solid-state packing effects as we recently discussed,[21] here our focus is on the electronic properties of the isolated molecules.

Polymethines typically have large negative $\mathrm{Re}(\gamma)$'s that very strongly increase in magnitude with backbone length as long as the molecular symmetry (C_{2v}) is maintained.[22,23] To understand this behavior, it is useful to consider the expression for molecular γ, written in terms of state energies and transition dipole moments in the framework of an essential-state model[24] derived from the sum-over-states (SOS) expression:[25]

$$\gamma \propto \frac{\mu_{ge}^2 \Delta\mu_{eg}^2}{(E_{ge} - \hbar\omega - i\Gamma_{ge})^2 (E_{ge} - 2\hbar\omega - i\Gamma_{ge})} \quad \mathbf{D}$$

$$+ \sum_{e'} \frac{\mu_{ge}^2 \mu_{ee'}^2}{(E_{ge} - \hbar\omega - i\Gamma_{ge})^2 (E_{ge'} - 2\hbar\omega - i\Gamma_{ge'})} \quad \mathbf{T}$$

$$- \frac{\mu_{ge}^4}{(E_{ge} - \hbar\omega - i\Gamma_{ge})^3} \quad \mathbf{N} \qquad (1)$$

Here, Γ_{ge} is a damping factor used to account for the broadening of the TPA spectrum. The ("dipolar") **D** term in the SOS expression is typically negligible for polymethines, as the difference between the state dipole moments of the ground and first excited state $\Delta\mu_{eg}$ is small. This then leaves contributions solely arising from the ("negative") **N** and ("two-photon") **T** terms. The large negative $\mathrm{Re}(\gamma)$ characteristic of polymethines originates from the inherently large transition dipole moment μ_{ge} between the ground and first excited states,[14] which is raised to the fourth power in the **N** term and therefore dominates the SOS expression. While many polymethines studied to date have large $|\mathrm{Re}(\gamma)|$, they also tend to have significant TPA that reduces the figure-of-merit.[26,27] This TPA dependence arises from the **T** term, which involves a sum over transitions from the first excited state to higher-lying TPA-allowed states, in particular the 2A state e'. Hence, when considering the design of molecular structures with **N** ≫ **T**, the contribution from the second excited state (e.g., $E_{ge'}$ and $\mu_{ee'}$) becomes the most significant characteristic to evaluate.

While it is generally found that the ratio of $E_{ge'}$ to E_{ge} is around 1.7,[28] the relationship between polymethine chemical structure and $\mu_{ee'}$ is not well understood. Although $\mu_{ee'}$ is small enough in some polymethines that the role of the **T** term in $\mathrm{Re}(\gamma)$ is negligible,[27−29] in other structures $\mu_{ee'}$ is comparable in magnitude to μ_{ge}.[12] Thus, it is important to better understand the relationship between chemical structure and $\mu_{ee'}$. Since the **T** term in the SOS expression for $\mathrm{Re}(\gamma)$ is positive,[25] a small $\mu_{ee'}$ aids in maximizing $|\mathrm{Re}(\gamma)|$; in addition, since the **T** term plays the most significant role in determining the $\mathrm{Im}(\gamma)$ magnitude, a small $\mu_{ee'}$ leads to a small TPA cross-section in state e', which helps keep $\mathrm{Im}(\gamma)$ small. We note, in contrast, that the **T** term for polyenes is typically larger than the **N** term, as the polyenes have many low-lying TPA states, resulting in a positive, smaller $\mathrm{Re}(\gamma)$.[14]

Achieving detailed insight into the structure−property relationships that affect $\mu_{ee'}$ is thus critical to the design of chromophores with improved NLO properties for AOS.[30] Here, we use electronic-structure methods to examine $\mu_{ee'}$ for a series of streptocyanines (i.e., polymethines with amino end substituents) and polyenes (Figure 1) that have long been used as model systems in computational and experimental studies of NLO response.[14,21,23,24,31] The molecular structures are varied in terms of the (i) conjugated path length and (ii) donor/acceptor substitution in the center of the molecular unit to evaluate effects common to the design of molecules for NLO response. We find that a key parameter determining the magnitude of $\mu_{ee'}$ is the energetic spacing among the first several frontier molecular orbitals, in particular the energetic gaps between the HOMO−1 and HOMO levels and the LUMO and LUMO+1 levels. As will be shown, the unique nodal patterns of the MOs in polymethines make donor/acceptor substitution in the center of the molecular unit a straightforward way of tuning the MO spacing. The insights gleaned in our theoretical study of substituent impacts on structure−property relationships are applicable to a much broader range of structural modifications to the polymethines.

METHODOLOGY

We first note that an important aspect from our calculations is to determine how the transition density changes as a function of molecular length and substitution. Just as a state dipole moment can be considered as a sum of contributions from the charge density associated with each atom, a transition dipole moment can be considered as a sum of contributions from the transition density at each atom, which is computed as the product of the wave functions of the initial and final states. In addition, since each wave function is a sum of contributions from the various electronic configurations, the transition dipole moment can be considered as a sum of contributions from each pair of initial and final electronic configurations. Hence, the decomposition of the transition dipole moments into (i) atomic transition densities and (ii) contributions from the component

dx.doi.org/10.1021/ph4001444 | ACS Photonics 2014, 1, 261−269

electronic configurations via the molecular orbitals and configuration interaction coefficients[32] provides a valuable tool to examine molecular structure effects on $\mu_{ee'}$. This insight will be used to gain a better handle on how common chemical modifications to polyenes and polymethines affect the NLO response. We note that the polymethines have very little geometric change upon excitation, as evidenced by the sharp absorption peaks with little vibronic structure in the experimental OPA and TPA spectra[28] and computed OPA spectra;[33,34] therefore, we have neglected vibronic effects and focused solely on the electronic components of the transition dipole moments.

The geometric structures of the polymethines and polyenes were optimized via density functional theory (DFT) with the ωB97X functional[35] and cc-pVDZ basis set[36] as implemented in the Gaussian 09 (Rev. B.01) suite of programs.[37] The excited-state properties were then evaluated using a configuration interaction (CI) approach with the INDO Hamiltonian;[14,32,38] this approach has previously provided excellent agreement with the experimental TPA properties of π-conjugated systems.[39,40] The CI active space included all single-electron (S) excitations within the 20 highest-lying occupied molecular orbitals (MOs) and 20 lowest-lying unoccupied MOs and all double-electron (D) excitations within the four highest-lying occupied MOs and four lowest-lying unoccupied MOs.[41]

The transition dipole moment $\mu_{ee'}$ between states e and e' is an off-diagonal matrix element of the dipole operator $\vec{\mu}$:

$$\mu_{ee'} = \langle \Psi_e | \vec{\mu} | \Psi_{e'} \rangle = \int \Psi_e^* e\vec{r} \Psi_{e'} d^3r = \int \rho_{e\to e'} e\vec{r} d^3r \tag{2}$$

where $\rho_{e\to e'}$ is the transition density between states e and e'. The total transition density and its decomposition into atomic and electronic-configuration components are determined using the CI coefficients and molecular orbitals from the INDO/SDCI calculations. The wave functions $|\Psi_e\rangle$ and $|\Psi_{e'}\rangle$ from the INDO/SDCI calculations are expressed as a sum of electronic configurations $|\psi_j\rangle$ with coefficients c_j:

$$|\Psi_e\rangle = \sum_j c_j |\psi_j\rangle \tag{3}$$

The electronic configurations are spin-adapted so that all the configurations are pure singlets:

$$\begin{aligned}
&\text{No unpaired electrons:} \quad |\psi_j\rangle = |...n\bar{n}o\bar{o}...\rangle \\
&\text{Two unpaired electrons:} \quad |\psi_j\rangle = \frac{1}{\sqrt{2}}(|...n\bar{n}o\bar{p}...\rangle - |...n\bar{n}\bar{o}p...\rangle) \\
&\text{Four unpaired electrons:} \quad |\psi_j\rangle = \frac{1}{2}(|...no\bar{p}\bar{q}...\rangle - |...n\bar{o}p\bar{q}...\rangle - |...\bar{n}o\bar{p}q...\rangle + |...\bar{n}\bar{o}pq...\rangle) \\
&\qquad\qquad |\psi_j\rangle = \frac{1}{2}(|...n\bar{o}p\bar{q}...\rangle - |...n\bar{o}\bar{p}q...\rangle - |...\bar{n}op\bar{q}...\rangle + |...\bar{n}o\bar{p}q...\rangle)
\end{aligned} \tag{4}$$

where n, o, p, and q are spin orbitals.

For each pair of electronic configurations, the transition dipole moment consists of an orbital component and a quantum prefactor. The orbital component can only be nonzero if the electronic configurations are no more than one orbital different. If the electronic configurations are one orbital different, the prefactor depends on both the number of unpaired electrons in each configuration and the orbitals between which the electron moves. As an example, we show below the calculation of the quantum prefactor for the $|H \to L\rangle \to |H,H \to L,L\rangle$ transition:

$$\begin{aligned}
&\langle H \to L | e\vec{r} | H, H \to L, L \rangle \\
&\quad = \frac{1}{\sqrt{2}}(\langle ...H\bar{L}...| - \langle ...\bar{H}L...|) e\vec{r} (|...L\bar{L}...\rangle) \\
&= \frac{1}{\sqrt{2}}(\langle ...H\bar{L}...|e\vec{r}|...L\bar{L}...\rangle) - \frac{1}{\sqrt{2}}(\langle ...\bar{H}L...|e\vec{r}|...L\bar{L}...\rangle) \\
&= \frac{1}{\sqrt{2}}(\langle ...H\bar{L}...|e\vec{r}|...L\bar{L}...\rangle) + \frac{1}{\sqrt{2}}(\langle ...L\bar{H}...|e\vec{r}|...L\bar{L}...\rangle) \\
&\qquad \text{Quantum prefactor} = \frac{1}{\sqrt{2}}(1+1) = \sqrt{2}
\end{aligned} \tag{5}$$

The orbital component of each transition dipole moment is determined by considering each molecular orbital as a sum of atomic orbitals φ_i with coefficients a_{ij}:

$$|\psi_j\rangle = \sum_i a_{ij} |\phi_i\rangle \tag{6}$$

and computed as a product of the two atomic orbital coefficients and the atomic positions $\vec{r}$ by assuming that the transition density between each pair of atomic orbitals is centered at the position of the atom and using the zero differential overlap approximation:

$$\begin{aligned}
\langle \psi_j | e\vec{r} | \psi_k \rangle &= \left(\sum_i a_{ij} \langle \phi_i |\right) e\vec{r} \left(\sum_l a_{lk} |\phi_l\rangle\right) \\
&= \sum_i \sum_l a_{ij} a_{lk} e\vec{r} \delta_{il} \\
&= \sum_i a_{ij} a_{ik} e\vec{r}
\end{aligned} \tag{7}$$

RESULTS AND DISCUSSION

We first discuss how changes to the chemical structure influence $\mu_{ee'}$ by investigating the influence of the conjugated path length in streptocyanines and in polyenes; we then turn to the impact of substitution with electron-rich and electron-deficient moieties.

1. Influence of the Conjugated Path Length: Streptocyanines. In the unsubstituted streptocyanine series (n = 1−5, Figure 1), the first excited state e is of B_2 symmetry and is dominated by the HOMO → LUMO (H → L) transition (CI contribution of 80−85%), as previously noted for polymethines.[14] The μ_{ge} value is large and increases with increasing molecular length (Table 1): as the HOMOs and LUMOs within the series extend over the full π system, lengthening the molecule allows the transition density to be large near both ends of the molecule, far from the molecular center. We note that the computed E_{ge} values fall within 0.2 eV of reported experimental absorption maxima for the longer streptocyanines, though E_{ge} is somewhat underestimated for the shortest cyanines; importantly, the μ_{ge} values are in reasonable agreement with the experimental oscillator strengths.[42,43]

dx.doi.org/10.1021/ph4001444 | ACS Photonics 2014, 1, 261−269

Table 1. Excited-State Energies (eV) and Transition Dipole Moments (Debye) for the Streptocyanines

molecular length (n)	E_{ge}	$E_{ge'}$	μ_{ge}	$\mu_{ee'}$
1	2.94	4.83	7.83	1.80
2	2.40	4.21	11.05	1.75
3	2.18	3.51	13.70	2.33
4	1.98	3.07	16.08	2.84
5	1.86	2.77	18.36	3.26

The second excited state e', on the other hand, is described by three electronic configurations: two single-electron excitations (H−1 → L and H → L+1) and one double-electron excitation (H, H → L, L). Since this state has A_1 symmetry, the transition from e to e' is one-photon-allowed.[44] However, $\mu_{ee'}$ is significantly smaller than μ_{ge}.

To understand the relatively small magnitude of $\mu_{ee'}$, we first consider the atomic transition densities. As shown in Figure 2,

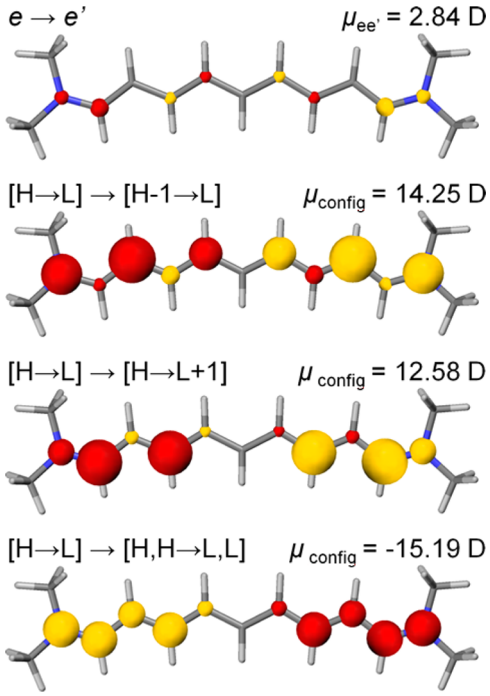

Figure 2. INDO/SDCI atomic transition densities and transition dipole moment $\mu_{ee'}$ as well as their major components for the (n = 4) streptocyanine. The areas of the circles are proportional to the transition densities associated with each atom; the color represents the phase of the transition density.

the atomic transition densities composing $\mu_{ee'}$ are small, a result that, at first sight, might appear to suggest poor orbital overlap in the transition. However, this is not the case, as all of the orbitals involved in the transition are π orbitals that extend across the molecular backbone (Figure 3).

In fact, it is useful to separate $\mu_{ee'}$ into the components coming from each of the three pairs of electronic configurations involved in the $e \rightarrow e'$ transition to understand how they individually contribute to the total transition dipole moment. The decomposition strategy reveals that three terms dominate $\mu_{ee'}$ in the streptocyanines; they correspond to the transitions from [H → L] in state e to each of the three main electronic configurations describing e'. Interestingly, any pure transition involving one of these three pairs of configurations has a large transition dipole moment, comparable in magnitude to μ_{ge}; see Figure 2. The key result, however, is that the transitions to the two singly excited configurations contribute to $\mu_{ee'}$ *with the same sign*, whereas the transition to the doubly excited configuration has a contribution *of opposite sign*. This partial cancellation of terms leads to $\mu_{ee'}$ being significantly smaller than μ_{ge}.

Another important result is that, as the streptocyanine length increases, both the transition dipole moments of the component transitions comprising $\mu_{ee'}$ and the CI contributions for each configuration in e' do change (see Figure 4), which determines the dependence of $\mu_{ee'}$ on molecular length. The transition dipole moments for each of the three pure transitions increase as the polymethine length increases since the relevant molecular orbitals extend along the entire molecular π system. The energetic spacing of the frontier MOs (going from the HOMO−1 level to the LUMO+1 level), shown in Figure 5, determines both the relative energies and CI contributions of the three component configurations in e'.[45] For the shortest streptocyanines, the energetic gap between the LUMO and LUMO+1 levels is slightly smaller than the energetic gaps between the HOMO and LUMO levels and between the HOMO−1 and HOMO levels; thus, [H → L+1] configurations have slightly smaller energies than the other two configurations and therefore have the largest CI contributions to the second excited state. As the molecular length increases, the first several frontier MOs become more evenly spaced, and the energy differences among the three configurations decrease. This leads to a decrease in the relative CI contribution of the [H → L+1] configuration and an increase in the contributions of the other configurations, particularly the doubly excited [H, H → L, L] configuration. We recall that, for all molecular lengths, the contributions of the two singly excited configurations to $\mu_{ee'}$ have the same sign, while the contribution of the doubly excited configuration has the opposite sign. Since the sum of the contributions of the single excitations decreases and the contribution of the double excitation increases, the change in the CI contributions results in significant cancellation and only modest increase in $\mu_{ee'}$ with increasing streptocyanine length. We note that if the CI contributions were constant with increasing length and only the component transition dipole moments changed, $\mu_{ee'}$ would increase by about 4 D as the length increased from n = 1 to n = 5, instead of the actual value of 1.46 D.

2. Influence of the Conjugated Path Length: Polyenes. As noted in the introduction, the ordering of the first two excited states in long polyenes is reversed relative to the polymethines: the $2A_g$ state e' is lower in energy than the $1B_u$ state e (Figure 1). Like in the streptocyanines, state e is primarily a H → L excitation and μ_{ge} is large (Table 2). State e' has significant contributions not only from the same three dominant excitations as in the streptocyanine state e' ([H−1 → L], [H → L+1], and [H, H → L, L]) but also (20−25%) from the double-electron excitation [H−1, H → L, L+1].[46] Since the transition dipole moment of a pure transition from [H → L] → [H−1, H → L, L+1] is substantially smaller than those of the other pure transitions, the contribution to $\mu_{ee'}$ is negligible and will not be considered further.

In the polyenes, all three of the pure transitions with a significant contribution to $\mu_{ee'}$ have transition dipole moments that increase with length; however, the [H → L] → [H, H → L, L] transition dipole moment has a weaker dependence on molecular length than the other two transitions (Figure 6). This

dx.doi.org/10.1021/ph4001444 | ACS Photonics 2014, 1, 261−269

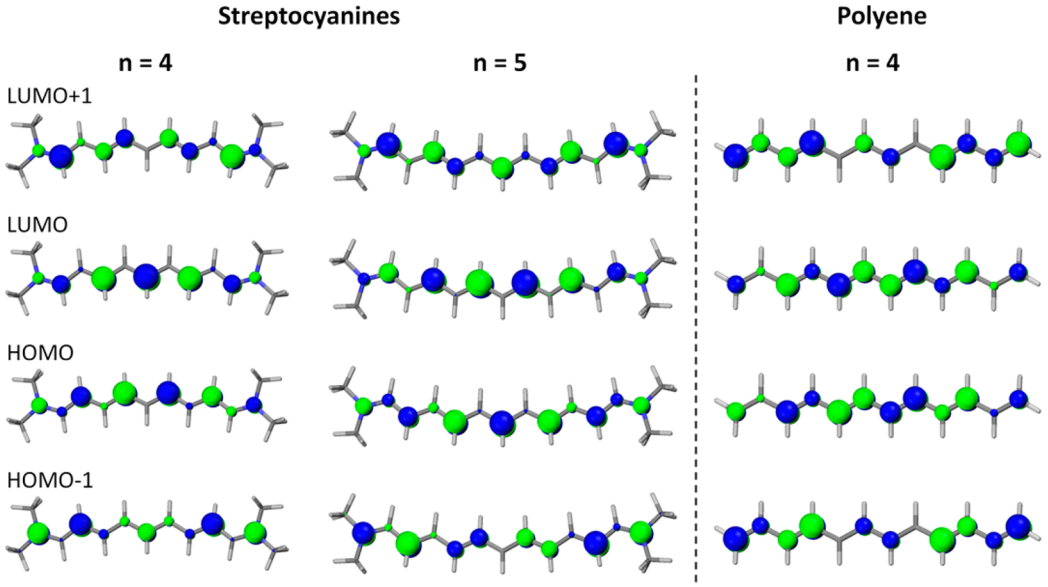

Figure 3. Frontier molecular orbitals of the streptocyanines and polyenes.

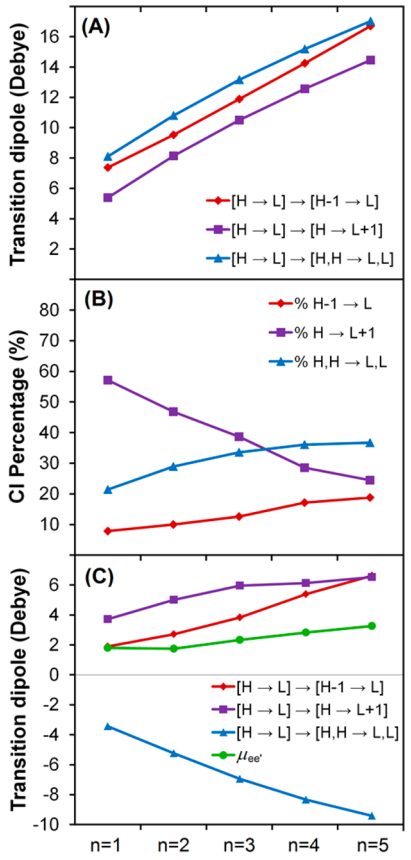

Figure 4. Evolution with streptocyanine length of (A) the transition dipole moments of the pure component transitions; (B) the CI contributions of the primary excitations in e'; and (C) $\mu_{ee'}$ and its major components.

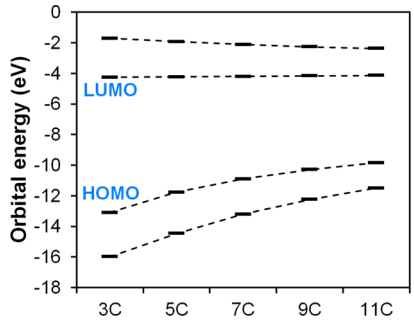

Figure 5. Energies of the streptocyanine frontier molecular orbitals at the INDO level.

Table 2. Excited-State Energies (eV) and Transition Dipole Moments (Debye) for Polyenes from Hexatriene (n = 1) to Tetradecaheptaene (n = 5)[a]

molecular length (n)	$E_{ge'}$	E_{ge}	$E_{ge''}$	$\mu_{ee'}$	μ_{ge}	$\mu_{ee''}$
1	4.69	6.11	8.70	2.30	6.00	12.3
2	4.49	5.48	7.86	3.93	7.57	14.4
3	4.46	5.19	7.38	3.48	9.10	18.1
4	4.18	4.94	6.76	4.39	10.6	20.3
5	4.00	4.44	6.30	5.39	11.8	22.3

[a]In these molecules, e' is the lowest excited state; see Figure 1.

is due primarily to the spatial distribution of the orbitals involved in the transition. The polyene HOMO and LUMO levels are more localized near the center of the molecule (Figure 3), whereas the HOMO−1 and LUMO+1 levels have larger contributions at the polyene ends; these trends become even more pronounced as the molecular length increases. Since the extent of the molecular orbitals involved in the [H → L] → [H, H → L, L] transition do not increase as rapidly as the molecular length, the corresponding transition dipole moment has an overall weaker length dependence; this is in contrast to the streptocyanines, where the molecular orbitals have a more even distribution along the entire molecular backbone, leading to more similar length dependences among the pure transition dipole moments.

As in the streptocyanines, the single excitations have contributions of the same sign to $\mu_{ee'}$, while the double excitation contributes with the opposite sign. In contrast, the CI contributions of the three electronic configurations contributing to the second excited states of the polyenes do not change significantly with length; as a result, $\mu_{ee'}$ increases linearly as the

dx.doi.org/10.1021/ph4001444 | ACS Photonics 2014, 1, 261−269

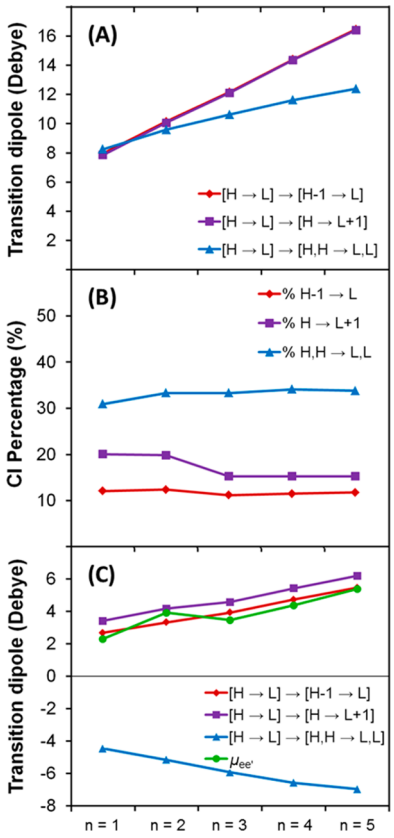

Figure 6. Evolution with polyene length of (A) the transition dipole moments of the pure component transitions; (B) the CI contributions of the primary excitations in e'; and (C) $\mu_{ee'}$ and its major components.

polyene length increases. Since $\mu_{ee'}$ is small in absolute value, the TPA cross-section of state e' is very small, in agreement with experimental observations.[17]

It is interesting to recall that computational[47−51] and experimental[17] evidence indicates that polyenes have a higher-lying mA_g state (e'') with a very significant TPA cross-section. The measured difference between the two-photon fluorescence activity of states e' and e'' in octatetraene[17] implies that $\mu_{ee''}$ is on the order of three times the magnitude of $\mu_{ee'}$.[52] With the same computational strategy as that used to understand the magnitude of $\mu_{ee'}$, we find that state e'' is primarily a linear combination of the same excitations that contribute to state e'; however, the sign of the double [H, H → L, L] excitation is reversed relative to that in state e', so all three transitions contribute to $\mu_{ee''}$ in the same manner. Hence, we arrive at the critical conclusion that $\mu_{ee''}$ in polyenes is large due to this additive effect rather than cancellation among the major contributing terms seen for $\mu_{ee'}$.

3. Influence of Electron-Donating (Methoxy) and -Withdrawing (Trifluoromethyl) Substituents. The dependence of $\mu_{ee'}$ on the molecular orbital energies suggests design principles that can be used to modulate $\mu_{ee'}$ by controlling the energetic spacings among the first few frontier molecular orbitals. If an electron-donating or electron-withdrawing substituent is added to the streptocyanine or polyene structures (here, a methoxy or a trifluoromethyl group), it primarily perturbs the energies of the molecular orbitals that have a significant weight of the wave function on the atom to which the substituent is bound. An important distinguishing feature between the polymethines and polyenes is that, in the case of the HOMO and LUMO levels, polymethines *can have nodes either on bonds or on carbon atoms*, whereas *nodes only exist on bonds* in polyenes. To address effects due to substitution with electron donors or acceptors while maintaining molecular symmetry, we have considered streptocyanines with one substituent on the central carbon atom and polyenes with substituents on the two central carbon atoms.

In polymethines, the π orbitals with an odd number of nodes have a node on the central carbon atom, while the remaining π orbitals have significant contribution to the wave function on the central carbon atom. In a streptocyanine containing n carbon−carbon double bonds, the HOMO has n+1 nodes (Figure 3); thus, the HOMO will have a node on the central carbon only if n is even. The LUMO+1 has the same *gerade* or *ungerade* symmetry as the HOMO, while the HOMO−1 and LUMO have the opposite symmetry. Due to this symmetry pattern, a substituent added to the central carbon atom of a streptocyanine where n is even primarily affects the HOMO−1 and LUMO orbital energies and has a much smaller effect on the HOMO and LUMO+1 energies; if n is instead odd, the pattern of which orbital energies are significantly affected is reversed.

The substituent has an important effect on the spacing of the polymethine frontier MOs. In particular, if n is even, an electron-withdrawing substituent stabilizes the HOMO−1 and LUMO, thereby narrowing the HOMO−LUMO gap but broadening the energetic spacing between the HOMO−1 and HOMO and between the LUMO and LUMO+1. This stabilizes the [H, H → L, L] excitation while having a smaller effect on the energies of the [H−1 → L] and [H → L+1] transitions. In this case, the coefficient of the double excitation in state e' increases, thereby decreasing $\mu_{ee'}$; see Figure 7. Conversely, if an electron-donating substituent is added in the same position, the HOMO−LUMO gap increases while the gaps between the HOMO−1 and HOMO and the LUMO and LUMO+1 decrease, thereby increasing $\mu_{ee'}$.

In contrast, if n is odd, a substituent on the central carbon atom primarily affects the HOMO and LUMO+1 energies, and the effect of the substituent on $\mu_{ee'}$ is reversed relative to the case where n is even. The stabilizing effect of the electron-withdrawing substituent in this case decreases the energetic spacing between the HOMO−1 and HOMO and the LUMO and LUMO+1, thus increasing $\mu_{ee'}$. The electron-donating substituent has the reverse effect and decreases $\mu_{ee'}$.

In the case of the polyenes, the frontier molecular orbitals have significant electron density on both central carbon atoms. Unlike in the polymethines, both electron-donating and electron-withdrawing substituents increase $\mu_{ee'}$ by 1−1.5 D and cause a slight reduction in the energetic spacing between the HOMO and HOMO−1. The contributions of the two single excitations to state e' increase with the addition of the substituents, with a corresponding decrease in the contribution of the [H−1, H → L, L+1] excitation. It must be noted that the trifluoromethyl substituents on the polyene result in a torsion angle of 140° instead of 180° around the central carbon−carbon bond; the energy-minimized geometry indicates that the torsion is related to energetically favorable hydrogen-bonding interactions between the fluorine and hydrogen atoms (H−F distances of 2.29 and 2.17 Å). Data from both the energetic minimum (solid lines) and a planar structure with one imaginary frequency (dotted lines) are shown in Figure 7 and

dx.doi.org/10.1021/ph4001444 | ACS Photonics 2014, 1, 261−269

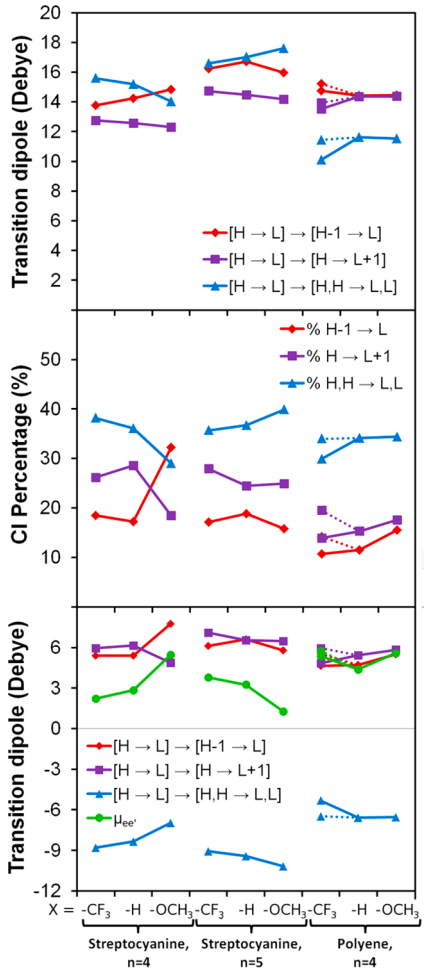

Figure 7. Evolution of $\mu_{ee'}$ and its major components with the addition of electron-donating and electron-withdrawing substituents to the (n = 4 and n = 5) streptocyanines and (n = 4) polyene.

reveal a fairly minor change to the pattern of $\mu_{ee'}$ as a function of the geometric difference.

These results highlight the critical feature of the energetic spacing of the frontier molecular orbital, which can be dictated by chemical substitution and the nodal patterns along the conjugated backbone, in determining the magnitude of $\mu_{ee'}$. The sign of the evolution in $\mu_{ee'}$ depends not on whether the substituent is electron-donating or electron-withdrawing but instead on how the substituent affects the molecular orbital energetic spacings. In particular, $\mu_{ee'}$ is small only when there is a large energetic spacing between the HOMO−1 and HOMO levels and the LUMO and LUMO+1 levels, which allows for nearly complete cancellation among the leading terms that contribute to $\mu_{ee'}$.

CONCLUSIONS

Evaluating the potential of third-order nonlinear optical materials requires a detailed understanding of the nature of the optical response beyond the first excited state, and in particular of the characteristics of the two-photon absorbing states. Although a large $\mu_{ee'}$ is critical for applications where two-photon absorption is desired, all-optical switching applications require a small $\mu_{ee'}$. Here, we have used a decomposition scheme to understand how the one- and two-electron configurations contributing to the e and e' states and the transitions between them ultimately determine the strength of $\mu_{ee'}$. While it has been noted[32] previously that $\mu_{ee'}$ is generally large when state e' consists primarily of one single-electron excitation and is smaller when state e' consists of a linear combination of single-electron and double-electron excitations, we have demonstrated how molecular structure, including effects of both conjugation length and substitution, influences the transition dipole moments of the individual electronic transitions that constitute $\mu_{ee'}$ in streptocyanines and polyenes.

The decomposition of $\mu_{ee'}$ indicates that its magnitude results from the interplay of two key factors: (i) the magnitudes of the pure component transition dipole moments that contribute to $\mu_{ee'}$, which relate to the spatial extent of the relevant frontier molecular orbitals (essentially from HOMO−1 to LUMO+1); and (ii) the contribution (CI coefficients) of each excitation to state e', resulting from the energetic spacing of the frontier molecular orbitals. In particular, to achieve a small $\mu_{ee'}$ in polymethines, the contribution of the [H, H → L, L] configuration in e' should be large, as it contributes in subtractive fashion to $\mu_{ee'}$. This can be accomplished by maintaining a large energy spacing between the HOMO−1 and HOMO levels and the LUMO and LUMO+1 levels, such that the three configurations with significant contributions to e' are comparable in energy. When electron-donating and electron-withdrawing moieties are substituted on the central portions of the conjugated backbones, our results demonstrate that the same substituent can either increase or decrease $\mu_{ee'}$ depending on the nodal patterns of the bridge-based frontier molecular orbitals.

The critical role of the energetic spacing of the frontier molecular orbitals in determining the magnitude of $\mu_{ee'}$ suggests design principles that can be applied as a broader range of structural modifications to the polymethines are considered. This is particularly true for potential end-group substituents, which have not been taken into account here. Such careful consideration should enable the design of chromophores with the large FOM critical for AOS applications. Efforts along these lines are currently being carried out in our laboratory.

ASSOCIATED CONTENT

Supporting Information

INDO molecular orbital energies, partial CI matrices derived from the INDO/SDCI calculations, and XYZ coordinates at the ωB97X/cc-pVDZ level. This information is available free of charge via the Internet at http://pubs.acs.org.

AUTHOR INFORMATION

Corresponding Author

*E-mail: jean-luc.bredas@chemistry.gatech.edu.

Present Address

[†]The Dow Chemical Company, Midland, Michigan 48674

Notes

The authors declare no competing financial interest.

ACKNOWLEDGMENTS

This work was supported by the AFOSR MURI program (FA9550-10-1-0558). We acknowledge stimulating discussions with Drs. S. Barlow, J. M Hales, S. R. Marder, and J. W. Perry.

REFERENCES

(1) Cisco visual networking index: Forecast and methodology, 2012−2017 (white paper), Cisco Systems, Inc., 2013. http://www.cisco.com/en/US/solutions/collateral/ns341/ns525/ns537/ns705/ns827/white_paper_c11-481360.pdf. June 10, 2013.

(2) Hinton, H. S. Switching to Photonics. *IEEE Spectrum* **1992**, *29*, 42−45.

(3) Albores-Meji, A.; Gomez-Agis, F.; Dorren, H. J. S.; Leijtens, X. J. M.; de Vries, T.; Oei, Y.-S.; Heck, M. J. R.; Notzel, R.; Robbins, D. J.; Smit, M. K.; Williams, K. A. Monolithic Multistage Optoelectronic Switch Circuit Routing 160 Gb/S Line-Rate Data. *J. Lightwave Technol.* **2010**, *28*, 2984−2992.

(4) Hochberg, M.; Baehr-Jones, T.; Wang, G.; Shearn, M.; Harvard, K.; Luo, J.; Chen, B.; Shi, Z.; Lawson, R.; Sullivan, P.; Jen, A. K. Y.; Dalton, L.; Scherer, A. Terahertz All-Optical Modulation in a Silicon−Polymer Hybrid System. *Nat. Mater.* **2006**, *5*, 703−709.

(5) Bahtiar, A.; Koynov, K.; Mardiyati, Y.; Hörhold, H.-H.; Bubeck, C. Slab Waveguides of Poly(p-Phenylenevinylene)s for All-Optical Switching: Impact of Side-Chain Substitution. *J. Mater. Chem.* **2009**, *19*, 7490.

(6) Koos, C.; Vorreau, P.; Vallaitis, T.; Dumon, P.; Bogaerts, W.; Baets, R.; Esembeson, B.; Biaggio, I.; Michinobu, T.; Diederich, F.; Freude, W.; Leuthold, J. All-Optical High-Speed Signal Processing with Silicon−Organic Hybrid Slot Waveguides. *Nat. Photonics* **2009**, *3*, 216−219.

(7) Stegeman, G. I.; Stolen, R. H. Waveguides and Fibers for Nonlinear Optics. *J. Opt. Soc. Am. B* **1989**, *6*, 652−662.

(8) Bredas, J. L.; Adant, C.; Tackx, P.; Persoons, A.; Pierce, B. M. Third-Order Nonlinear Optical Response in Organic Materials: Theoretical and Experimental Aspects. *Chem. Rev.* **1994**, *94*, 243−278.

(9) Marks, T. J.; Ratner, M. A. Design, Synthesis, and Properties of Molecule-Based Assemblies with Large Second-Order Optical Nonlinearities. *Angew. Chem., Int. Ed. Engl.* **1995**, *35*, 155−173.

(10) Bartholomew, G. P.; Ledoux, I.; Mukamel, S.; Bazan, G. C.; Zyss, J. Three-Dimensional Nonlinear Optical Chromophores Based on Through-Space Delocalization. *J. Am. Chem. Soc.* **2002**, *2002*, 13480−13485.

(11) Bouit, P.-A.; Wetzel, G.; Berginc, G.; Loiseaux, B.; Toupet, L.; Feneyrou, P.; Bretonniere, Y.; Kamada, K.; Maury, O.; Andraud, C. Near IR Nonlinear Absorbing Chromophores with Optical Limiting Properties at Telecommunication Wavelengths. *Chem. Mater.* **2007**, *19*, 5325−5335.

(12) Padilha, L. A.; Webster, S.; Przhonska, O. V.; Hu, H.; Peceli, D.; Ensley, T. R.; Bondar, M. V.; Gerasov, A. O.; Kovtun, Y. P.; Shandura, M. P.; Kachkovski, A. D.; Hagan, D. J.; Van Stryland, E. W. Efficient Two-Photon Absorbing Acceptor-Pi-Acceptor Polymethine Dyes. *J. Phys. Chem. A* **2010**, *114*, 6493−6501.

(13) Dalton, L. R.; Benight, S. J.; Johnson, L. E.; Knorr, D. B.; Kosilkin, I.; Eichinger, B. E.; Robinson, B. H.; Jen, A. K. Y.; Overney, R. M. Systematic Nanoengineering of Soft Matter Organic Electro-Optic Materials. *Chem. Mater.* **2011**, *23*, 430−445.

(14) Meyers, F.; Marder, S. R.; Pierce, B. M.; Bredas, J. L. Electric Field Modulated Nonlinear Optical Properties of Donor-Acceptor Polyenes: Sum-over-States Investigation of the Relationship between Molecular Polarizabilities (Alpha, Beta, and Gamma) and Bond Length Alternation. *J. Am. Chem. Soc.* **1994**, *116*, 10703−10714.

(15) Marder, S. R.; Gorman, C. B.; Meyers, F.; Perry, J. W.; Bourhill, G.; Brédas, J. L.; Pierce, B. M. A Unified Description of Linear and Nonlinear Polarization in Organic Polymethine Dyes. *Science* **1994**, *265*, 632−635.

(16) Hudson, B. S.; Kohler, B. E. A Low-Lying Weak Transition in the Polyene Alpha,Omega-Diphenyloctatetraene. *Chem. Phys. Lett.* **1972**, *14*, 299−304.

(17) Kohler, B. E.; Terpougov, V. Octatetraene M 1ag States: Two-Photon Fluorescence Excitation Spectrum from 28000 to 50000 cm^{-1}. *J. Chem. Phys.* **1996**, *104*, 9297.

(18) Kohler, B. E.; Terpougov, V. Electronic States of Linear Polyenes: High Resolution Spectroscopy of Cis- and Trans-1,3,5,7,9-Decapentaene. *J. Chem. Phys.* **1998**, *108*, 9586.

(19) Angeli, C.; Pastore, M. The Lowest Singlet States of Octatetraene Revisited. *J. Chem. Phys.* **2011**, *134*, 184302.

(20) Kogej, T.; Beljonne, D.; Meyers, F.; Perry, J. W.; Marder, S. R.; Bredas, J.-L. Mechanisms for Enhancement of Two-Photon Absorption in Donor−Acceptor Conjugated Chromophores. *Chem. Phys. Lett.* **1998**, *298*, 1−6.

(21) Mukhopadhyay, S.; Risko, C.; Marder, S. R.; Brédas, J.-L. Polymethine Dyes for All-Optical Switching Applications: A Quantum-Chemical Characterization of Counter-ion and Aggregation Effects on the Third-Order Nonlinear Optical Response. *Chem. Sci.* **2012**, *3*, 3103.

(22) Tolbert, L. M.; Zhao, X. Beyond the Cyanine Limit: Peierls Distortion and Symmetry Collapse in a Polymethine Dye. *J. Am. Chem. Soc.* **1997**, *119*, 3253−3258.

(23) Wernke, W.; Pfeiffer, M.; Johr, T.; Lau, A.; Grahn, W.; Johannes, H.-H.; Dahne, L. Increase and Saturation of the Third Order Hyperpolarizabilities in Homologous Series of Symmetric Cyanines. *Chem. Phys.* **1997**, *216*, 337−347.

(24) Pierce, B. M. A Theoretical Analysis of the Third-Order Nonlinear Optical Properties of Linear Cyanines and Polyenes. *Proc. SPIE* **1991**, *1560*, 148−161.

(25) Orr, B. J.; Ward, J. F. Perturbation Theory of the Non-linear Optical Polarization of an Isolated System. *Mol. Phys.* **1971**, *20*, 513−526.

(26) Hales, J. M.; Zheng, S.; Barlow, S.; Marder, S. R.; Perry, J. W. Bisdioxaborine Polymethines with Large Third-Order Nonlinearities for All-Optical Signal Processing. *J. Am. Chem. Soc.* **2006**, *128*, 11362−11363.

(27) Hales, J. M.; Matichak, J.; Barlow, S.; Ohira, S.; Yesudas, K.; Bredas, J. L.; Perry, J. W.; Marder, S. R. Design of Polymethine Dyes with Large Third-Order Optical Nonlinearities and Loss Figures of Merit. *Science* **2010**, *327*, 1485−1488.

(28) Fu, J.; Padilha, L. A.; Hagan, D. J.; Van Stryland, E. W.; Przhonska, O. V.; Bondar, M. V.; Slominsky, Y. L.; Kachkovskii, A. Molecular Structure − Two-Photon Absorption Property Relations in Polymethine Dyes. *J. Opt. Soc. Am. B* **2007**, *24*, 56−66.

(29) Matichak, J. D.; Hales, J. M.; Barlow, S.; Perry, J. W.; Marder, S. R. Dioxaborine- and Indole-Terminated Polymethines: Effects of Bridge Substitution on Absorption Spectra and Third-Order Polarizabilities. *J. Phys. Chem. A* **2011**, *115*, 2160−2168.

(30) Gieseking, R. L.; Mukhopadhyay, S.; Risko, C.; Marder, S. R.; Brédas, J.-L. 25th Anniversary Article: Design of Polymethine Dyes for All-Optical Switching Applications: Guidance from Theoretical and Computational Studies. *Adv. Mater.* **2014**, *26*, 68−84.

(31) Johr, T.; Wernke, W.; Pfeiffer, M.; Lau, A.; Dahne, L. Third-Order Nonlinear Polarizabilities of a Homologous Series of Symmetric Cyanines. *Chem. Phys. Lett.* **1995**, *246*, 521−526.

(32) Zojer, E.; Beljonne, D.; Kogej, T.; Vogel, H.; Marder, S. R.; Perry, J. W.; Brédas, J. L. Tuning the Two-Photon Absorption Response of Quadrupolar Organic Molecules. *J. Chem. Phys.* **2002**, *116*, 3646.

(33) Guillaume, M.; Liégeois, V.; Champagne, B.; Zutterman, F. Time-Dependent Density Functional Theory Investigation of the Absorption and Emission Spectra of a Cyanine Dye. *Chem. Phys. Lett.* **2007**, *446*, 165−169.

(34) Mustroph, H.; Reiner, K.; Mistol, J.; Ernst, S.; Keil, D.; Hennig, L. Relationship between the Molecular Structure of Cyanine Dyes and the Vibrational Fine Structure of Their Electronic Absorption Spectra. *ChemPhysChem* **2009**, *10*, 835−840.

(35) Chai, J.-D.; Head-Gordon, M. Systematic Optimization of Long-Range Corrected Hybrid Density Functionals. *J. Chem. Phys.* **2008**, *128*, 084106.

(36) Dunning, T. H. Gaussian Basis Sets for Use in Correlated Molecular Calculations. I. The Atoms Boron through Neon and Hydrogen. *J. Chem. Phys.* **1989**, *90*, 1007.

(37) Frisch, M. J.; Trucks, G. W.; Schlegel, H. B.; Scuseria, G. E.; Robb, M. A.; Cheeseman, J. R.; Scalmani, G.; Barone, V.; Mennucci, B.; Petersson, G. A.; Nakatsuji, H.; Caricato, M.; Li, X.; Hratchian, H. P.; Izmaylov, A. F.; Bloino, J.; Zheng, G.; Sonnenberg, J. L.; Hada, M.;

Ehara, M.; Toyota, K.; Fukuda, R.; Hasegawa, J.; Ishida, M.; Nakajima, T.; Honda, Y.; Kitao, O.; Nakai, H.; Vreven, T.; Montgomery, J. A., Jr.; Peralta, J. E.; Ogliaro, F.; Bearpark, M.; Heyd, J. J.; Brothers, E.; Kudin, K. N.; Staroverov, V. N.; Keith, T.; Kobayashi, R.; Normand, J.; Raghavachari, K.; Rendell, A.; Burant, J. C.; Iyengar, S. S.; Tomasi, J.; Cossi, M.; Rega, N.; Millam, J. M.; Klene, M.; Knox, J. E.; Cross, J. B.; Bakken, V.; Adamo, C.; Jaramillo, J.; Gomperts, R.; Stratmann, R. E.; Yazyev, O.; Austin, A. J.; Cammi, R.; Pomelli, C.; Ochterski, J. W.; Martin, R. L.; Morokuma, K.; Zakrzewski, V. G.; Voth, G. A.; Salvador, P.; Dannenberg, J. J.; Dapprich, S.; Daniels, A. D.; Farkas, O.; Foresman, J. B.; Ortiz, J. V.; Cioslowski, J.; Fox, D. J. *Gaussian 09*, Revision B.01; Gaussian, Inc.: Wallingford, CT, 2010.

(38) Ohira, S.; Hales, J. M.; Thorley, K. J.; Anderson, H. L.; Perry, J. W.; Bredas, J. L. A New Class of Cyanine-Like Dyes with Large Bond-Length Alternation. *J. Am. Chem. Soc.* **2009**, *131*, 6099−6101.

(39) Zojer, E.; Beljonne, D.; Pacher, P.; Bredas, J. L. Two-Photon Absorption in Quadrupolar Pi-Conjugated Molecules: Influence of the Nature of the Conjugated Bridge and the Donor-Acceptor Separation. *Chem.—Eur. J.* **2004**, *10*, 2668−2680.

(40) Zojer, E.; Wenseleers, W.; Halik, M.; Grasso, C.; Barlow, S.; Perry, J. W.; Marder, S. R.; Brédas, J.-L. Two-Photon Absorption in Linear Bis-Dioxaborine Compounds—the Impact of Correlation-Induced Oscillator-Strength Redistribution. *ChemPhysChem* **2004**, *5*, 982−988.

(41) For the two shortest polyenes, the active space was reduced to 15 HOMOs and 15 LUMOs. Although excited-state energies can sometimes change significantly with changing the size of the active space or moving from an SDCI to an MRDCI approach, the transition dipoles are much less affected.

(42) Malhotra, S. S.; Whiting, M. C. 756. Researches on Polyenes. Part VII. The Preparation and Electronic Absorption Spectra of Homologous Series of Simple Cyanines, Merocyanines, and Oxonols. *J. Chem. Soc.* **1960**, 3812.

(43) Fabian, J.; Hartmann, H. *Light Absorption of Organic Colorants*; Springer-Verlag: Heidelberg, 1980.

(44) Because of the C_{2v} symmetry, the transition from state g to state e' is symmetry-allowed only along the short molecular axis and $\mu_{ge'}$ is negligibly small.

(45) The exact INDO energies for each transition are provided along with the partial CI matrices in the Supporting Information.

(46) Since this electronic configuration has four unpaired electrons, there are two singlet configurations that both contribute to the polyene state e'. Consideration of the orbital overlap would imply that the pure transition dipole moment for a transition from H → L to H−1, H → L, L+1 is roughly half that of the other excitations with large contributions to $\mu_{ee'}$; however, since the two singlets have contributions of opposite signs to $\mu_{ee'}$, the effective transition dipole moment is substantially smaller.

(47) Dixit, S.; Guo, D.; Mazumdar, S. Essential-States Mechanism of Optical Nonlinearity in π-Conjugated Polymers. *Phys. Rev. B* **1991**, *43*, 6781−6784.

(48) Mazumdar, S.; Guo, D.; Dixit, S. N. High Energy Two-Photon States in Finite versus Infinite Polyenes. *J. Chem. Phys.* **1992**, *96*, 6862.

(49) Luo, Y.; Agren, H.; Stafstrom, S. One- and Two-Photon Absorption Spectra of Short Conjugated Polyenes. *J. Phys. Chem.* **1994**, *98*, 7782−7789.

(50) Beljonne, D.; Shuai, Z.; Serrano-Andres, L.; Brédas, J. L. The Dominant One- and Two-Photon Excited States in the Nonlinear Optical Response of Octatetraene: Ab Initio versus Semiempirical Theoretical Descriptions. *Chem. Phys. Lett.* **1997**, *279*, 1−8.

(51) Knippenberg, S.; Rehn, D. R.; Wormit, M.; Starcke, J. H.; Rusakova, I. L.; Trofimov, A. B.; Dreuw, A. Calculations of Nonlinear Response Properties Using the Intermediate State Representation and the Algebraic-Diagrammatic Construction Polarization Propagator Approach: Two-Photon Absorption Spectra. *J. Chem. Phys.* **2012**, *136*, 064107.

(52) According to ref 15, the measured two-photon fluorescence is 63 times greater for state e'' than for state e'. Given that the two-photon fluorescence activity is directly proportional to Im(γ) when $2\hbar\omega$ is equal to the state energy, the experimental state energies and two-photon fluorescence activities can be used to approximate the ratio of $\mu_{ee''}$ to $\mu_{ee'}$ via the **T** term in the SOS expression (eq 1).